

NASA Technical Memorandum 106373  
ICOMP-93-37

IN-34  
193181  
11P

# Multigrid Time-Accurate Integration of Navier-Stokes Equations

Andrea Arnone  
*Institute for Computational Mechanics in Propulsion*  
*Lewis Research Center*  
*Cleveland, Ohio*

*and University of Florence*  
*Florence, Italy*

and

Meng-Sing Liou and Louis A. Povinelli  
*National Aeronautics and Space Administration*  
*Lewis Research Center*  
*Cleveland, Ohio*

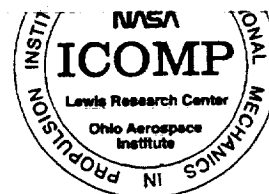
(NASA-TM-106373) MULTIGRID  
TIME-ACCURATE INTEGRATION OF  
NAVIER-STOKES EQUATIONS (NASA)  
11 p

N94-17258

Unclass

G3/34 0193181

November 1993



+1.5

# MULTIGRID TIME-ACCURATE INTEGRATION OF NAVIER-STOKES EQUATIONS

Andrea Arnone\*  
Institute for Computational Mechanics in Propulsion  
Lewis Research Center  
Cleveland, Ohio 44135

and University of Florence  
Florence, Italy

and

Meng-Sing Liou† and Louis A. Povinelli‡  
National Aeronautics and Space Administration  
Lewis Research Center  
Cleveland, Ohio 44135

## Abstract

Efficient acceleration techniques typical of explicit steady-state solvers are extended to time-accurate calculations. Stability restrictions are greatly reduced by means of a fully implicit time discretization. A four-stage Runge-Kutta scheme with local time stepping, residual smoothing, and multigriding is used instead of traditional time-expensive factorizations. Some applications to natural and forced unsteady viscous flows show the capability of the procedure.

## Introduction

Recent progress in Computational Fluid Dynamics along with the evolution of computer performance is encouraging scientists to look at the details of flow physics more and more. There are a variety of practical applications where the unsteadiness of the problem can not be neglected (i.e. vortex shedding, natural unsteadiness, forced unsteadiness, aeroelasticity, turbomachinery rotor-stator interaction). Up to now, in several branches of engineering most of the analysis and designing tools are based on a steady or quasi-steady assumption, even if the flow is known to be unsteady. Today, due to the improvement in computer resources, there is a strong interest in developing methodologies for efficient and reliable simulation of unsteady flow features.

It is a common experience, while using time accurate explicit schemes, to be forced to choose the time step on the basis of stability restrictions. As a consequence, unless the problem is a very high frequency one, the number of time steps to be performed is much higher than the one required for time accuracy.

By means of some implicit factorization, most of the stability restrictions can be removed, but the work required at each time step grows rapidly with grid dimension and complexity of the flow equations. In addition, several boundary conditions can be difficult to treat in a fully implicit way.

In viscous flow calculations, the grid is stretched close to the shear layer and the characteristic time step varies several orders of magnitude inside the computational domain. Even if in practical applications the characteristic time step of the core-flow region is comparable with the one suggested by accuracy, close to the walls the time step restrictions are very severe. Therefore highly vectorizable schemes with less stability restrictions on the allowable time step would be an interesting combination.

Explicit schemes with accelerating techniques have proven to be very effective for solving steady problems<sup>1,2,3</sup>. Unfortunately, the computational efficiency of those time-marching solvers is achieved by sacrificing the accuracy in time. In this paper, we present a procedure to show that the conventional steady-state acceleration techniques, specifically the multigrid techniques, can still be applied to unsteady Navier-Stokes problems as well, while still achieving efficiency. The basic idea is to reformulate the governing equations so that they can be handled by an explicit accelerated scheme<sup>4</sup>. If the time discretization is made implicit, stability restrictions are removed and accelerating techniques can be used instead of traditional time-expensive factorizations (i.e. ADI, LU).

As one of the final goals of the present research will be the study of unsteady phenomena in turbomachinery components, such as rotor-stator interaction and stage analysis, we implemented the technique in the TRAF(2D/3D) codes<sup>3,5</sup>. These two- and three-dimensional solvers were developed during a joint project between the University of Florence and NASA Lewis and were designed for turbomachinery blade row analysis.

\* Assistant Professor, Department of Energy Engineering

† Senior Scientist, Internal Fluid Mechanics Division, Member AIAA

‡ Deputy Chief, Internal Fluid Mechanics Division, Member AIAA

The procedure is validated by applying it to some examples of natural and forced unsteady two-dimensional viscous flows.

### Governing Equations

Let  $t, \rho, u, v, p, T, E$ , and  $H$  denote respectively time, density, the absolute velocity components in the  $x$  and  $y$  Cartesian directions, pressure, temperature, specific total energy, and specific total enthalpy. The two-dimensional, unsteady, Reynolds-averaged Navier-Stokes equations can be written for a moving grid in conservative form in a curvilinear coordinate system  $\xi, \eta$  as,

$$\frac{\partial(J^{-1}Q)}{\partial t} + \frac{\partial F}{\partial \xi} + \frac{\partial G}{\partial \eta} = \frac{\partial F_v}{\partial \xi} + \frac{\partial G_v}{\partial \eta} \quad (1)$$

where,

$$Q = \begin{Bmatrix} \rho \\ \rho u \\ \rho v \\ \rho E \end{Bmatrix}, F = J^{-1} \begin{Bmatrix} \rho U \\ \rho u U + \xi_x p \\ \rho v U + \xi_y p \\ \rho H U + \xi_t p \end{Bmatrix}, G = J^{-1} \begin{Bmatrix} \rho V \\ \rho u V + \eta_x p \\ \rho v V + \eta_y p \\ \rho H V - \eta_t p \end{Bmatrix} \quad (2)$$

The contravariant velocity components of eqs. (2) are written as,

$$U = \xi_t + \xi_x u + \xi_y v, \quad V = \eta_t + \eta_x u + \eta_y v \quad (3)$$

and the transformation metrics are defined by,

$$\begin{aligned} \xi_x &= J y_\eta, & \xi_y &= J x_\eta, & \xi_t &= -x_t \xi_x - y_t \xi_y \\ \eta_x &= J y_\xi, & \eta_y &= J x_\xi, & \eta_t &= -x_t \eta_x - y_t \eta_y \end{aligned} \quad (4)$$

where the Jacobian of the transformation  $J$  is,

$$J^{-1} = x_\xi y_\eta - x_\eta y_\xi \quad (5)$$

The viscous flux terms are assembled in the form,

$$F_v = J^{-1} \begin{Bmatrix} 0 \\ \xi_x \tau_{xx} + \xi_y \tau_{xy} \\ \xi_x \tau_{yx} + \xi_y \tau_{yy} \\ \xi_x \beta_x + \xi_y \beta_y \end{Bmatrix}, \quad G_v = J^{-1} \begin{Bmatrix} 0 \\ \eta_x \tau_{xx} + \eta_y \tau_{xy} \\ \eta_x \tau_{yx} + \eta_y \tau_{yy} \\ \eta_x \beta_x + \eta_y \beta_y \end{Bmatrix} \quad (6)$$

where,

$$\tau_{xx} = 2\mu u_x + \lambda(u_x + v_y)$$

$$\begin{aligned} \tau_{yy} &= 2\mu v_y + \lambda(u_x + v_y) \\ \tau_{xy} = \tau_{yx} &= \mu(u_y + v_x) \\ \beta_x &= u \tau_{xx} + v \tau_{xy} + k T_x \\ \beta_y &= u \tau_{yx} + v \tau_{yy} + k T_y \end{aligned} \quad (7)$$

and the Cartesian derivatives of (7) are expressed in terms of  $\xi$ - and  $\eta$ -derivatives using the chain rule, i.e.,

$$u_x = \xi_x u_\xi + \eta_x u_\eta \quad (8)$$

The pressure is obtained from the equation of state,

$$p = \rho R T \quad (9)$$

According to the Stokes hypothesis,  $\lambda$  is taken to be  $-2\mu/3$  and a power law is used to determine the molecular coefficient of viscosity  $\mu$  as function of temperature. The eddy-viscosity hypothesis is used to account for the effect of turbulence. The molecular viscosity  $\mu$  and the molecular thermal conductivity  $k$  are replaced with,

$$\mu = \mu_l + \mu_t \quad (10)$$

$$k = c_p \left[ \left( \frac{\mu}{Pr} \right)_l + \left( \frac{\mu}{Pr} \right)_t \right] \quad (11)$$

where  $c_p$  is the specific heat at constant pressure,  $Pr$  is the Prandtl number, and the subscripts  $l$  and  $t$  refer to laminar and turbulent quantities respectively. The turbulent quantities  $\mu_t$  and  $Pr_t$  are computed using the two-layer mixing length model of Baldwin and Lomax<sup>6</sup>.

### Spatial Discretization and Artificial Dissipation

Traditionally, using a finite-volume approach, the governing equations are discretized in space starting from an integral formulation and without any intermediate mapping. In the present work, due to the large use of eigenvalues and curvilinear quantities, we found it more convenient to map the Cartesian space  $(x, y)$  in a generalized curvilinear one  $(\xi, \eta)$ . In the curvilinear system, the equation of motion (1) can be easily rewritten in integral form by means of Green's theorem and the metric terms are handled following the standard finite-volume formulation. A cell-centered scheme is used to store the flow variables. On each cell face the convective and diffusive fluxes are calculated after computing the necessary flow quantities at the face center. Those quantities are obtained by a simple averaging of adjacent cell-center values of the dependent variables.

In viscous calculations, dissipating properties are present due to diffusive terms. Away from the shear layer regions, the physical diffusion is generally not sufficient to prevent the odd-even point decoupling of centered schemes. Thus, to maintain stability and to prevent oscillations near shocks or stagnation points, artificial dissipation terms are also included in the viscous calculations. Equation (1) is written in semi-discrete form as,

$$\frac{\partial Q}{\partial t} + C(Q) - D(Q) = 0 \quad (14)$$

where the discrete operator  $C$  accounts for the physical convective and diffusive terms, while  $D$  is the operator for the artificial dissipation. The artificial dissipation model used in this paper is basically the one originally introduced by Jameson, Schmidt, and Turkel<sup>7</sup>. In order to minimize the amount of artificial diffusion inside the shear layer, the eigenvalues scalings of Martinelli and Jameson<sup>8</sup>, and Swanson and Turkel<sup>9</sup> have been used to weight these terms. The quantity  $D(Q)$  in eq. (14) is defined as,

$$D(Q) = (D_\xi^2 - D_\xi^4 + D_\eta^2 - D_\eta^4)Q \quad (15)$$

where, for example, in the  $\xi$  curvilinear coordinates we have,

$$\begin{aligned} D_\xi^2 Q &= \nabla_\xi (\Lambda_{i+1/2,j} \epsilon_{i+1/2,j}^{(2)}) \Delta_\xi Q_{i,j} \\ D_\xi^4 Q &= \nabla_\xi (\Lambda_{i+1/2,j} \epsilon_{i+1/2,j}^{(4)}) \Delta_\xi \nabla_\xi \Delta_\xi Q_{i,j} \end{aligned} \quad (16)$$

$i, j$  are indices associated with the  $\xi, \eta$  directions and  $\nabla_\xi, \Delta_\xi$  are forward and backward difference operators in the  $\xi$  direction. The variable scaling factor  $\Lambda$  is defined as,

$$\Lambda_{i+1/2,j} = \frac{1}{2} \left[ (\Lambda_\xi)_{i,j} + (\Lambda_\xi)_{i+1,j} \right] \quad (17)$$

and,

$$\Lambda_\xi = \Phi_\xi \lambda_\xi \quad (18)$$

$$\Phi_\xi = 1 + \left( \frac{\lambda_\eta}{\lambda_\xi} \right)^\sigma \quad (19)$$

where  $\lambda_\xi$  and  $\lambda_\eta$  are the scaled spectral radii of the flux Jacobian matrices for the convective terms,

$$\lambda_\xi = |U| + a \sqrt{\xi_x^2 + \xi_y^2}, \quad \lambda_\eta = |V| + a \sqrt{\eta_x^2 + \eta_y^2} \quad (20)$$

and  $a$  is the speed of sound. Note that the effect of the grid motion is accounted for in (20) through the definition of the contravariant components of velocities of (3). The exponent  $\sigma$  is generally defined by  $0 < \sigma \leq 1$ , and for two-dimensional applications, a value of  $2/3$  gives satisfactory results. The coefficients  $\epsilon^{(2)}$  and  $\epsilon^{(4)}$  use the pressure as a sensor for shocks and stagnation points, and are defined as follows,

$$\epsilon_{i+1/2,j}^{(2)} = K^{(2)} \text{MAX}(v_{i-1,j}, v_{i,j}, v_{i+1,j}, v_{i+2,j}) \quad (21)$$

$$v_{i,j} = \frac{p_{i-1,j} - 2p_{i,j} + p_{i+1,j}}{p_{i-1,j} + 2p_{i,j} + p_{i+1,j}} \quad (22)$$

$$\epsilon_{i+1/2,j}^{(4)} = \text{MAX} \left[ 0, (K^{(4)} - \epsilon_{i+1/2,j}^{(2)}) \right] \quad (23)$$

where typical values for the constants  $K^{(2)}$  and  $K^{(4)}$  are  $1/2$  and  $1/64$  respectively. For the other direction,  $\eta$ , the contribution of dissipation is defined in a similar way. The computation of the dissipating terms is carried out in each coordinate direction as the difference between first and third difference operators. Those operators are set to zero on solid walls in order to reduce the global error on the conservation property and to prevent the presence of undamped modes<sup>9,10</sup>.

### Boundary Conditions

In cascade-like configurations there are four different types of boundaries: inlet, outlet, solid wall, and periodicity. According to the theory of characteristics, the flow angle, total pressure, total temperature, and isentropic relations are used at the subsonic-axial inlet, while the outgoing Riemann invariant is taken from the interior. At the subsonic-axial outlet, the average value of the static pressure is prescribed and the density and components of velocity are extrapolated.

On the solid walls, the pressure is extrapolated from the interior points, and the no-slip condition and the temperature condition are used to compute density and total energy. For the calculations presented in this paper, all the walls have been assumed to be at a constant temperature equal to the total inlet one.

Cell-centered schemes are generally implemented using phantom cells to handle the boundaries. The periodicity is, therefore, easily overimposed by setting periodic phantom cell values. On the boundaries where the grid is not periodic, the phantom cells overlap the real ones. Linear interpolations are then used to compute the value of the dependent variables in phantom cells.

**Basic Time-Stepping Scheme and Acceleration Techniques for the Steady Problem**

The system of the differential equation (14) is advanced in time using an explicit four-stage Runge-Kutta scheme until the steady-state solution is reached. A hybrid scheme is implemented, where, for economy, the viscous terms are evaluated only at the first stage and then frozen for the remaining stages. If  $l$  is the index associated with time we will write it in the form,

$$\begin{aligned}
 Q^{(0)} &= Q' \\
 Q^{(1)} &= Q^{(0)} + \alpha_1 R(Q^{(0)}) \\
 Q^{(2)} &= Q^{(0)} + \alpha_2 R(Q^{(1)}) \\
 Q^{(3)} &= Q^{(0)} + \alpha_3 R(Q^{(2)}) \\
 Q^{(4)} &= Q^{(0)} + \alpha_4 R(Q^{(3)}) \\
 Q^{j+1} &= Q^{(4)} \\
 \alpha_1 &= \frac{1}{4}, \quad \alpha_2 = \frac{1}{3}, \quad \alpha_3 = \frac{1}{2}, \quad \alpha_4 = 1
 \end{aligned} \tag{24}$$

where the residual  $R(Q)$  is defined by,

$$R(Q) = \Delta t J [C(Q) - D(Q)] \tag{25}$$

Good, high-frequency damping properties, important for the multigrid process, have been obtained by performing two evaluations of the artificial dissipating terms, at the first and second stages.

In order to reduce the computational cost, three techniques are employed to speed up convergence to the steady state-solution. These techniques: 1) local time-stepping; 2) residual smoothing; 3) multigrid; are briefly described in the following.

**Local Time-Stepping**

For steady state calculations, a faster expulsion of disturbances can be achieved by locally using the maximum allowable time step. In the present work the local time step limit  $\Delta t$  is computed accounting for both the convective ( $\Delta t_c$ ) and diffusive ( $\Delta t_d$ ) contributions as follows,

$$\Delta t = c_0 \left( \frac{\Delta t_c \Delta t_d}{\Delta t_c + \Delta t_d} \right) \tag{26}$$

where  $c_0$  is a constant usually taken to be the Courant-Friedrichs-Lewy (CFL) number. Specifically, for the inviscid and viscous time step we used,

$$\Delta t_c = \frac{l}{\lambda_\xi + \lambda_\eta} \tag{27}$$

$$\Delta t_d = \frac{l}{K_t \frac{\gamma \mu}{\rho Pr} J^2 (S_\xi^2 + S_\eta^2)} \tag{28}$$

where  $\gamma$  is the specific heat ratio and,

$$S_\xi^2 = x_\xi^2 + y_\xi^2, \quad S_\eta^2 = x_\eta^2 + y_\eta^2 \tag{29}$$

$K_t$  being a constant whose value has been set equal to 2.5 based on numerical experiments.

**Residual Smoothing**

An implicit smoothing of residuals is used to extend the stability limit and the robustness of the basic scheme. This technique was first introduced by Lerat<sup>11</sup> in 1979 in conjunction with Lax-Wendroff type schemes. Later, in 1983, Jameson<sup>1</sup> implemented it on the Runge-Kutta stepping scheme. In two dimensions, the residual smoothing is carried out in the form,

$$(1 - \beta_\xi \nabla_\xi \Delta_\xi)(1 - \beta_\eta \nabla_\eta \Delta_\eta) \tilde{R} = R \tag{30}$$

where the residual  $R$  includes the contribution of the variable time step and is defined by (25) and  $\tilde{R}$  is the residual after a sequence of smoothing in the  $\xi$ , and  $\eta$ , directions with coefficients  $\beta_\xi$ , and  $\beta_\eta$ . For viscous calculations on highly stretched meshes the variable coefficient formulations of Martinelli and Jameson<sup>8</sup> and Swanson and Turkel<sup>9</sup> have proven to be robust and reliable. In the present paper, the expression for the variable coefficients  $\beta$  of (30) has been implemented as follows,

$$\begin{aligned}
 \beta_\xi &= \text{MAX} \left\{ 0, \frac{1}{4} \left[ \left( \frac{CFL}{CFL^*} \frac{\lambda_\xi}{\lambda_\xi + \lambda_\eta} \Phi_\xi \right)^2 - 1 \right] \right\} \\
 \beta_\eta &= \text{MAX} \left\{ 0, \frac{1}{4} \left[ \left( \frac{CFL}{CFL^*} \frac{\lambda_\eta}{\lambda_\xi + \lambda_\eta} \Phi_\eta \right)^2 - 1 \right] \right\}
 \end{aligned} \tag{31}$$

where the coefficients  $\Phi_\xi$  and  $\Phi_\eta$  are the ones defined in eqs. (19), and  $CFL$ , and  $CFL^*$  are the Courant numbers of the smoothed and unsmoothed scheme respectively. For the hybrid four-stage scheme we used  $CFL=5$ , and  $CFL^*=2.5$ .

### Multigrid

This technique was developed in the beginning of the 1970s for the solution of elliptic problems<sup>12</sup> and later was extended to time-dependent formulations<sup>1,2</sup>. The basic idea is to introduce a sequence of coarser grids and to use them to speed up the propagation of the fine grid corrections, resulting in a faster expulsion of disturbances. In this work, the Full Approximation Storage (FAS) schemes of Brandt<sup>12</sup> and Jameson<sup>1</sup> is used.

Coarser, auxiliary meshes are obtained by doubling the mesh spacing and the solution is defined on them using a rule which conserves mass, momentum, and energy,

$$\left(J^{-1}Q^{(0)}\right)_{2h} = \sum \left(J^{-1}Q\right)_h \quad (32)$$

where the subscripts refer to the grid spacing, and the sum is over the eight cells which compose the  $2h$  grid cell. Note that this definition coincides with the one used by Jameson<sup>1</sup> when the reciprocal of the Jacobians are replaced with the cell volumes. To respect the fine grid approximation, forcing functions  $P$  are defined on the coarser grids and added to the governing equations. So, after the initialization of  $Q_{2h}$  using eq.(32), forcing functions  $P_{2h}$  are defined as,

$$P_{2h} = \sum R_h(Q_h) - R_{2h}(Q_{2h}^{(0)}) \quad (33)$$

and added to the residuals  $R_{2h}$  to obtain the value  $R_{2h}^*$  which is then used for the stepping scheme.

$$R_{2h}^* = R_{2h}(Q_{2h}) + P_{2h} \quad (34)$$

This procedure is repeated on a succession of coarser grids and the corrections computed on each coarse grid are transferred back to the finer one by bilinear interpolations.

A V-type cycle with subiterations is used as a multigrid strategy. The process is advanced from the fine grid to the coarser one without any intermediate interpolation, and when the coarser grid is reached, corrections are passed back. One Runge-Kutta step is performed on the  $h$  grid, two on the  $2h$  grid, and three on all the coarser grids.

For viscous flows with very low Reynolds number or strong separation, it is important to compute the viscous terms on the coarse grids, too. The turbulent viscosity is evaluated only on the finest grid level and then interpolated on coarse grids.

On each grid, the boundary conditions are treated in the same way and updated at every Runge-Kutta stage. For economy, the artificial dissipation model is replaced on the coarse grids with constant coefficient second-order differences. On coarse grids, the turbulent

viscosity is evaluated by averaging the surrounding fine grid values.

### Reformulation of the Governing Equations

Explicit Runge-Kutta schemes in conjunction with residual smoothing and multigrid have proven to be very efficient for steady problems, however those time-dependent methods are no longer time accurate. As shown by Jameson<sup>4</sup> for the Euler equations, the system of (1) can be reformulated to be handled by a time-marching steady-state solver. The equations (1) and (14) are rewritten in a compact form as,

$$\frac{\partial Q}{\partial t} = -\mathcal{R}(Q) \quad (35)$$

where  $\mathcal{R}$  is the residual which includes convective, diffusive, and artificial dissipation fluxes. By the introduction of a fictitious time  $\tau$  the unsteady governing equations can be reformulated and a new residual  $\mathcal{R}^*$  defined as,

$$\frac{\partial Q}{\partial \tau} = \frac{\partial Q}{\partial t} + \mathcal{R}(Q) = \mathcal{R}^*(Q) \quad (36)$$

now  $\tau$  is a fictitious time and all the accelerating techniques developed in steady-state experiences, can be used to efficiently reduce the new residual  $\mathcal{R}^*$ , while marching in  $\tau$ . Following the approach of Jameson<sup>4</sup>, derivatives with respect to the real time  $t$  are discretized using a three-point backward formula which results in an implicit scheme which is second order accurate in time,

$$\frac{\partial Q}{\partial \tau} = \frac{3Q^{n+1} - 4Q^n + Q^{n-1}}{2\Delta t} + \mathcal{R}(Q^{n+1}) = \mathcal{R}^*(Q^{n+1}) \quad (37)$$

where the superscript  $n$  is associated with the real time. Between each time step the solution is advanced in a non-physical time  $\tau$  and acceleration strategies like local time stepping, implicit residual smoothing, and multigriding are used to speed up the residual  $\mathcal{R}^*$  to zero to satisfy the time-accurate equations.

The time discretization of (37) is fully implicit, however, when solved by marching in  $\tau$  stability problems can occur when the stepping in the fictitious time  $\tau$  exceeds the physical one. This generally occurs in viscous calculations where core-flow cells are much bigger than those close to shear-layer. Based on a linear stability analysis of the four-stage scheme of (24) applied to (37), the stepping in  $\tau$  must be less than  $2/3 CFL^* \Delta t$ . The time step  $\Delta \tau$  can then be corrected as follows,

$$\Delta \tau = \text{MIN} \left( \Delta \tau, \frac{\Delta t}{2^{m-1} \frac{3}{2} \frac{CFL}{CFL^*}} \right) \quad (38)$$

where the contribution of the multigrid speed-up is included through  $2^{m-1}$ ,  $m$  being the total number of grids used in the multigrid process. After limiting the time step  $\Delta \tau$  with (38) the scheme becomes stable and the physical time step  $\Delta t$  can be chosen safely only on the basis of the accuracy requirement.

At the end of each time step in real time, the time derivative  $\partial Q / \partial t$  is updated and a new sequence in the fictitious time  $\tau$  is started. From 10 to 20 multigrid cycles are typically needed between time steps.

To provide a good initialization of the solution at the new time step, a three-point backward formula is used as a predictor,

$$Q^* = Q^n + \frac{3Q^n - 4Q^{n-1} + Q^{n-2}}{2} \quad (39)$$

where  $Q^*$  is the predicted value of  $Q^{n+1}$ .

We stress that, using scheme (37), the modifications to turn an existing steady-solution solver to a time accurate one are quite simple. The time derivative  $\partial Q / \partial t$  can be introduced as a source term to be included in the new residual  $\mathcal{R}^*$ , and the time step is corrected using eq. (38) to make the scheme stable.

### Results and Discussions

In this very first part of the research project the procedure is validated in two-dimensions. Three test cases are presented. Firstly, a vortex shedding over a row of circular cylinders in a laminar regime is examined. The interest being mostly in the flow periodicity and in the prediction of the Strouhal number. As a second application of natural unsteadiness, a shock buffeting over a row of bicircular airfoils will be discussed. Finally, the last application is related to forced unsteadiness in turbomachines and simulates the effect of passing stator wakes on a rotor blade.

#### Row of Circular Cylinders

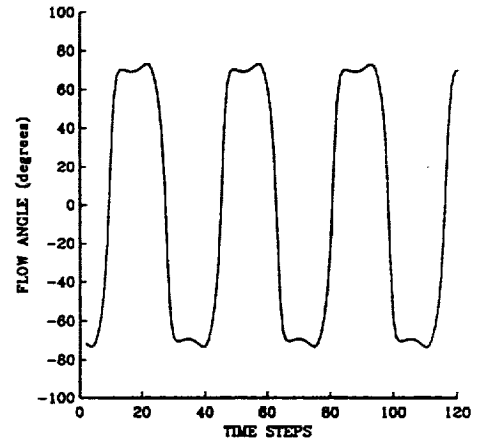
This test is intended to predict the natural vortex shedding past a cylinder. A row of circular cylinders in a laminar regime is studied for an inlet flow condition of Mach number 0.2 and Reynolds number of 1000. Calculations were performed on a  $257 \times 49$  elliptic C-type grid. The distance between the cylinders is five times the cylinder diameter.

Figures 1(a) and (b) report the evolution in time of the flow angle and velocity components (phase plot) at a

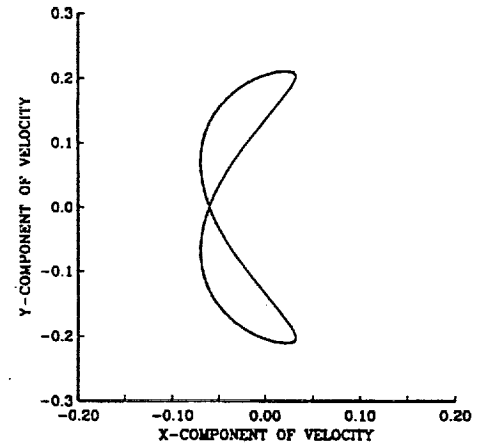
point in the wake close to the cylinder. The time history refers to four cycles of oscillations after a periodic flow condition is reached. The very periodic behaviour of the flow is evident and proves the robustness and accuracy of the scheme. The time step for those calculations was set to have 40 divisions over a cycle. This corresponds to a local Courant number between three (far field) and four hundred (boundary layer).

The computed Strouhal number based on the inlet velocity is about 0.2 and agrees well with the experimental value of 0.21.

Figure 2 reports the instantaneous particle traces in nine instants over a cycle (the tenth position would be equivalent to the first). The shedding of the vortex is very evident as well as the mechanism of their formation with a vortex merging between instants 1 and 2, and 5 and 6.



a) flow angle evolution



b) velocity component evolution

Fig. 1. Unsteady flow past a circular cylinder ( $M=0.2, Re=100$ ).

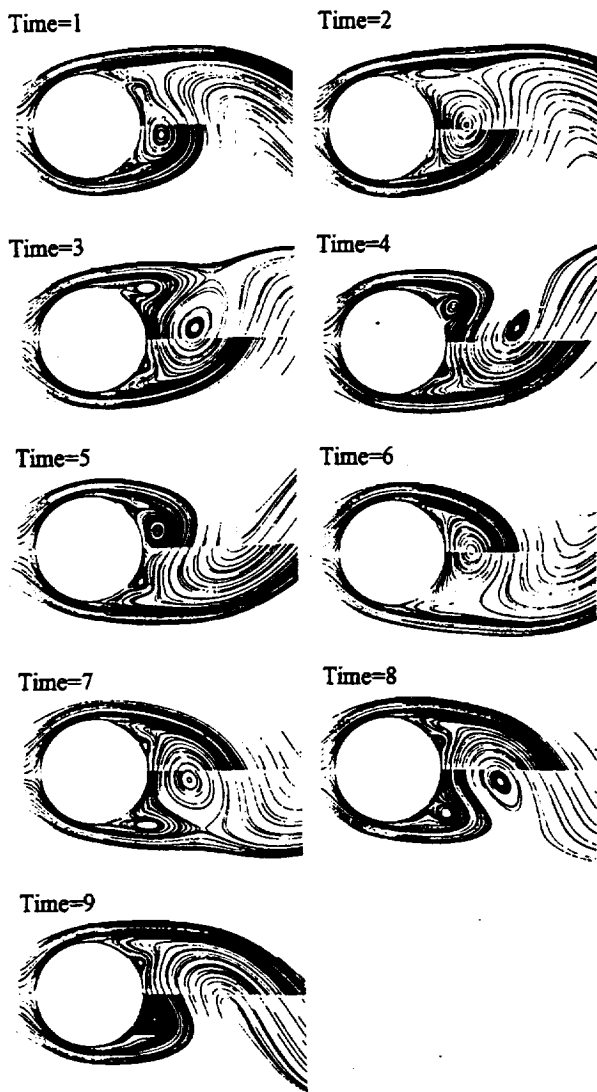
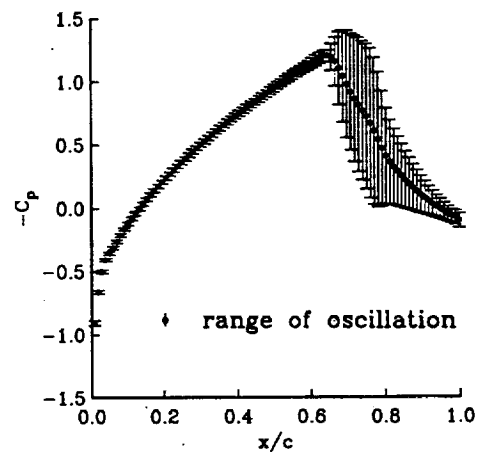


Fig. 2. Instantaneous particle traces for the circular cylinder row test case

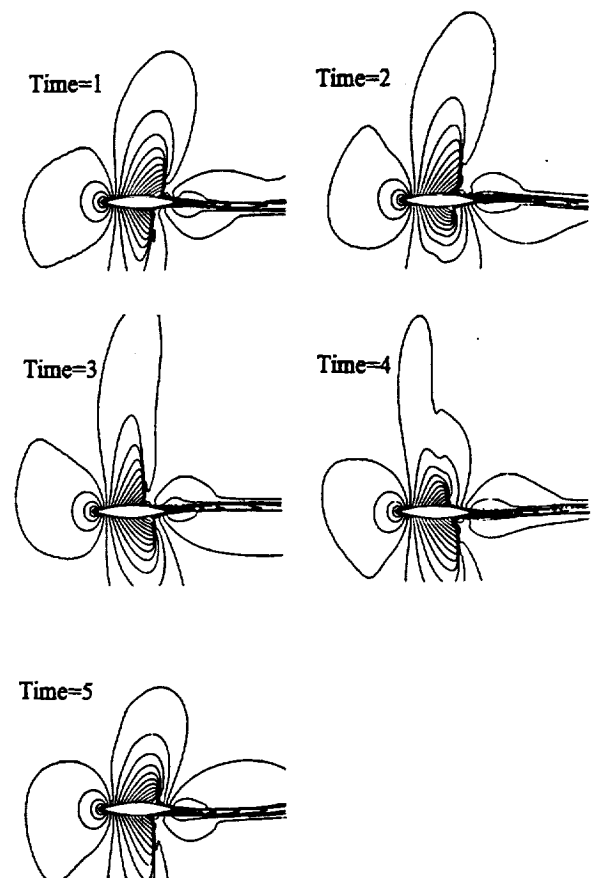
### Shock Buffeting Over a Bicircular Airfoil

Starting from about 1976 several experiments and calculations were carried out on shock buffeting over a bicircular-arc airfoil. The experiments<sup>13,14</sup> were carried out at NASA Ames in a wind tunnel designed for this purpose. At a Reynolds number of 7 million, experiments suggest buffeting at a free stream Mach number in the range from 0.74 to 0.76. In agreement, the present calculations indicate natural unsteady flow at Mach 0.75. On the contrary, while, the flow is experimented to be unsteady up to a Mach number of 0.78, the calculation still shows some unsteadiness up to a free stream Mach number of 0.83. The nominal test Mach number for the experiments is 0.775 and the wind tunnel endwalls were designed to minimize wall effects for this flow condition.

Far away from the nominal condition, endwall effects become important especially at high Mach numbers and so the comparison with a row of airfoils becomes not too meaningful.



a) pressure coefficient distribution



b) instantaneous Mach number contours

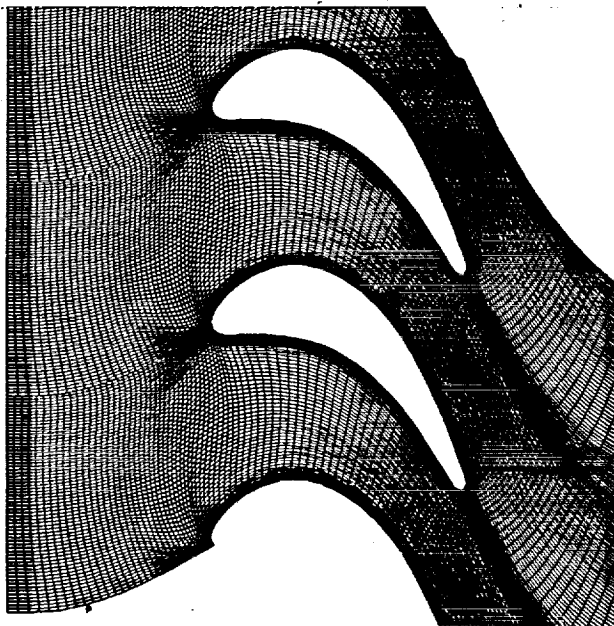
Fig. 3. Shock buffeting over a row of bicircular-arc airfoils ( $M=0.775$ ,  $Re=7 \times 10^6$ )

The reduced frequency of the experiment is roughly 0.5. Steger<sup>15</sup>, with an isolated airfoil predicted about 0.41, while the TRAF2D code suggested 0.42 for an airfoil distance of ten times the axial cord. If the airfoils are clustered to a distance of four times the axial cord, the reduced frequency rises to 0.47, once again suggesting some influence of existing walls on the buffeting frequency.

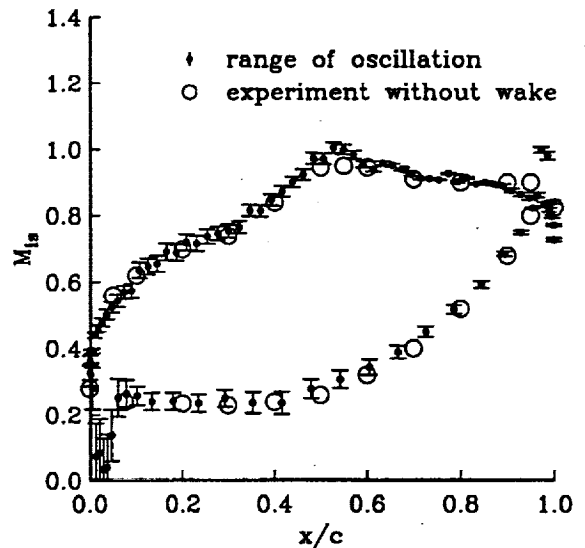
Instantaneous Mach number contours are reported in Fig. 3 along with the range of pressure distribution. For that high Reynolds number the Courant number based on forty divisions within a cycle was between one (far field) and three thousand (boundary layer). The grid used is an H-type (153x97) and a buffeting cycle requires about 8 minutes on the NASA Lewis Cray Y-MP.

### Passing Wakes Effects on a Rotor Blade

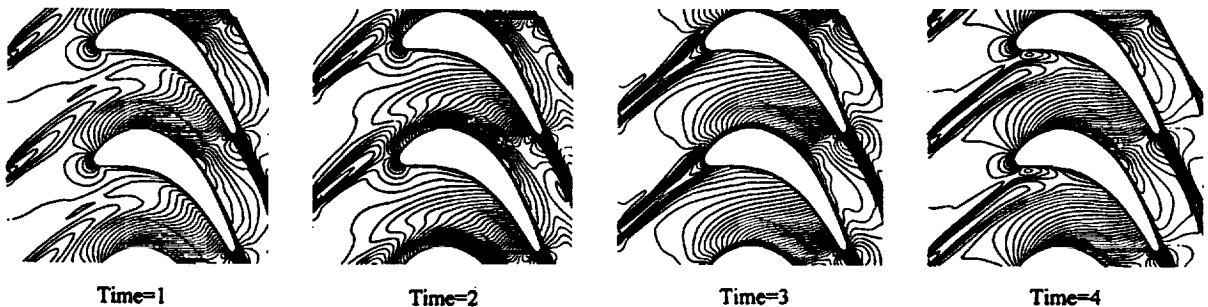
As a preliminary application to unsteady effects in turbomachinery, a rotor configuration with incoming moving wakes, was studied. A H-type grid (see Fig. 4(a)) was selected in order to minimize the incoming wake smearing due to grid coarsening. The wake is simulated with a loss in total pressure and an alteration in the velocity direction. Figure 4(b) shows the isentropic Mach number range on the blade surface. The wind tunnel data<sup>16</sup> without wake effects are also reported. The instantaneous Mach number contours are given in Fig. 4 (c) in terms of four instants over a cycle.



a) 129x65 elliptic H-type grid



b) isentropic Mach number distribution on the blade surface



c) instantaneous Mach number contours

Fig. 4. Passing wakes effect on a rotor blade ( $M_{2is}=.81$ ,  $Re_2=.8 \times 10^6$ )

### Conclusions

The use of explicit accelerated schemes has been extended to time-accurate Navier-Stokes calculations. Particularly the use of efficient and highly vectorizable techniques such as multigriding is proposed in conjunction with a fully implicit time discretization. A preliminary validation indicates that the approach is robust and efficient. According to the proposed method, the modifications to be made on a time-marching accelerated solver in order to make it time accurate are very simple.

### Acknowledgements

The first author would like to express his gratitude to ICOMP and NASA for providing support, facilities, and computer time for this work. Thanks are also due to Prof. Sergio S. Stecco of the University of Florence, for encouraging the research.

### References

1. Jameson, A., 1983 " Transonic Flow Calculations, " MAE Report 1651, MAE Department, Princeton University.
2. Ni, R-H, 1981 " A Multiple-Grid Scheme for Solving the Euler Equations, " AIAA paper 81-1025.
3. Arnone, A., Liou, M.-S., and Povinelli, L. A., 1991, " Multigrid Calculation of Three-Dimensional Viscous Cascade Flows, " AIAA paper 91-3238.
4. Jameson, A., 1991, "Time Dependent Calculations Using Multigrid, with Applications to Unsteady Flows Past Airfoils and Wings," AIAA Paper 91-1596.
5. Arnone, A., and Swanson, R. C., 1988 " A Navier-Stokes Solver for Cascade Flows, " NASA CR No. 181682.
6. Baldwin, B. S., and Lomax, H., 1978 "Thin Layer Approximation and Algebraic Model for Separated Turbulent Flows, " AIAA paper 78-257.
7. Jameson, A., Schmidt, W., and Turkel, E., 1981 " Numerical Solutions of the Euler Equations by Finite Volume Methods Using Runge-Kutta Time-Stepping Schemes, " AIAA paper 81-1259.
8. Martinelli, L. and Jameson, A., 1988 " Validation of a Multigrid Method for the Reynolds Averaged Equations, " AIAA paper 88-0414.
9. Swanson, R. C., and Turkel, E., 1987 " Artificial Dissipation and Central Difference Schemes for the Euler and Navier-Stokes Equations., " AIAA paper 87-1107.
10. Pulliam, T. H., 1986 " Artificial Dissipation Models for the Euler Equations, " *AIAA Journal*, Vol. 24, No. 12, December, pp. 1931-1940.
11. Lerat, A., 1979 " Une Classe de Schemas aux Differences Implicites Pour les Systemes Hyperboliques de Lois de Conservation, " *Comptes Rendus Acad. Sciences Paris*, Vol. 288 A.
12. Brandt, A., 1979 " Multi-Level Adaptive Computations in Fluid Dynamics, " AIAA paper 79-1455.
13. Levy, L. L., 1977, "An Experimental and Computational Investigation of the Steady and Unsteady Transonic Flow Field About an Airfoil in a Solid-Wall Test Channel," AIAA Paper 77-678.
14. McDevitt, J. B., Levy, L. L., and Deiwert, G. S., 1976, " Transonic Flow About a Thick Circular-Arc Airfoil, " *AIAA Journal*, Vol. 14, No. 5, May 1976, pp. 606-613.
15. Steger, J. L., 1978, " Implicit Finite-Difference Simulation of Flow About Arbitrary Two-Dimensional Geometries, " *AIAA Journal*, Vol. 16, No. 7, July 1978, pp. 679-686.
16. Sieverding, C. H., 1973, " Experimental Data on Two Transonic Turbine Blade Sections and Comparison with Various Theoretical Methods," VKI Report, LS59 (1973).

# REPORT DOCUMENTATION PAGE

Form Approved  
OMB No. 0704-0188

Public reporting burden for this collection of information is estimated to average 1 hour per response, including the time for reviewing instructions, searching existing data sources, gathering and maintaining the data needed, and completing and reviewing the collection of information. Send comments regarding this burden estimate or any other aspect of this collection of information, including suggestions for reducing this burden, to Washington Headquarters Services, Directorate for Information Operations and Reports, 1215 Jefferson Davis Highway, Suite 1204, Arlington, VA 22202-4302, and to the Office of Management and Budget, Paperwork Reduction Project (0704-0188), Washington, DC 20503.

<b>1. AGENCY USE ONLY (Leave blank)</b>		<b>2. REPORT DATE</b> November 1993	<b>3. REPORT TYPE AND DATES COVERED</b> Technical Memorandum	
<b>4. TITLE AND SUBTITLE</b>  Multigrid Time-Accurate Integration of Navier-Stokes Equations			<b>5. FUNDING NUMBERS</b>  WU-505-90-5K	
<b>6. AUTHOR(S)</b>  Andrea Arnone, Meng-Sing Liou, and Louis A. Povinelli				
<b>7. PERFORMING ORGANIZATION NAME(S) AND ADDRESS(ES)</b>  National Aeronautics and Space Administration Lewis Research Center Cleveland, Ohio 44135-3191			<b>8. PERFORMING ORGANIZATION REPORT NUMBER</b>  E-8183	
<b>9. SPONSORING/MONITORING AGENCY NAME(S) AND ADDRESS(ES)</b>  National Aeronautics and Space Administration Washington, D.C. 20546-0001			<b>10. SPONSORING/MONITORING AGENCY REPORT NUMBER</b>  NASA TM-106373 ICOMP-93-37	
<b>11. SUPPLEMENTARY NOTES</b> Andrea Arnone, Institute for Computational Mechanics in Propulsion, NASA Lewis Research Center and University of Florence, Florence, Italy; Meng-Sing Liou and Louis A. Povinelli, NASA Lewis Research Center, (work funded under NASA Cooperative Agreement NCC3-233). ICOMP Program Director, Louis A. Povinelli, (216) 433-5818.				
<b>12a. DISTRIBUTION/AVAILABILITY STATEMENT</b>  Unclassified - Unlimited Subject Categories 34 and 64			<b>12b. DISTRIBUTION CODE</b>	
<b>13. ABSTRACT (Maximum 200 words)</b>  Efficient acceleration techniques typical of explicit steady-state solvers are extended to time-accurate calculations. Stability restrictions are greatly reduced by means of a fully implicit time discretization. A four-stage Runge-Kutta scheme with local time stepping, residual smoothing, and multigriding is used instead of traditional time-expensive factorizations. Some applications to natural and forced unsteady viscous flows show the capability of the procedure.				
<b>14. SUBJECT TERMS</b>  Multigrid; Navier-Stokes equations; Unsteady flow			<b>15. NUMBER OF PAGES</b> 10	
			<b>16. PRICE CODE</b> A02	
<b>17. SECURITY CLASSIFICATION OF REPORT</b> Unclassified	<b>18. SECURITY CLASSIFICATION OF THIS PAGE</b> Unclassified	<b>19. SECURITY CLASSIFICATION OF ABSTRACT</b> Unclassified	<b>20. LIMITATION OF ABSTRACT</b>	